CARBON letters

Original Articles
Carbon Letters Vol. 27, 35-41 (2018)

Single-walled carbon nanotubes directly-grown from orientated carbon nanorings

Tomohiro Tojo[1,♠], Ryoji Inada[1], Yoji Sakurai[1] and Yoong Ahm Kim[2,♠]

[1]Department of Electrical and Electronic Information Engineering, Toyohashi University of Technology, Toyohashi 441-8580, Japan
[2]Department of Polymer Engineering, Graduate School, School of Polymer Science and Engineering & Alan G. MacDiarmid Energy Research Institute, Chonnam National University, Gwangju 61186, Korea

Article Info
Received 28 November 2017
Accepted 17 January 2018

♠Corresponding Author
E-mail: tojo@ee.tut.ac.jp
yak@chonnam.ac.kr
Tel: +81-532-44-6728
Tel: +82-62-530-1871

Open Access
DOI: http://dx.doi.org/10.5714/CL.2018.27.035

This is an Open Access article distributed under the terms of the Creative Commons Attribution Non-Commercial License (http://creativecommons.org/licenses/by-nc/3.0/) which permits unrestricted non-commercial use, distribution, and reproduction in any medium, provided the original work is properly cited.

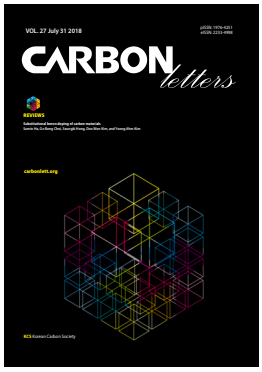

http://carbonlett.org

pISSN: 1976-4251
eISSN: 2233-4998

Copyright © Korean Carbon Society

Abstract

Surfactant-wrapped separation methods of metallic and semiconducting single-walled carbon nanotubes (SWCNTs) can result in large changes in intrinsic physical and chemical properties due to electronic interactions between a nanotube and a surfactant. Our approach to synthesize SWCNTs with an electronic feature relied on utilizing carbon nanorings, [*n*]cycloparaphenylenes ([*n*]CPPs), which are the fundamental unit of armchair type SWCNTs (a-SWCNTs) that possess a metallic feature without any surfactants. To obtain long tubular structures from [*n*]CPPs, the host-guest complexes formed with well-aligned [*n*]CPP hosts and various fullerene guests on a silicon substrate were pyrolyzed under an ethanol gas flow at a high temperature with focused-ultraviolet laser irradiation. The pyrolyzed [*n*]CPPs were observed to transform from nanorings to tubular structures with 1.5–1.7 nm diameters corresponding to the employed diameter of [*n*]CPPs. Our approach suggests that [*n*]CPPs are useful for structure-controlled synthesis of SWCNTs.

Key words: chirality, cycloparaphenylenes, fullerenes, single-walled carbon nanotubes

1. Introduction

Recently, metallic and semiconducting single-walled carbon nanotubes (SWCNTs) have gained much attention as nanomaterials in electronics and photonics, such as transistors [1,2], sensors [3,4], transparent conductive films [5-7], and photovoltaic cells [8,9] due to substantial carrier mobility, high sensitivity, and high chemical/mechanical stability. Since their electronic features strongly depend on the diameter and side wall structure (i.e., chirality), the chirality control approach is very important for several promising applications. Although a few physical and chemical approaches (e.g., gas phase etching [10], chemical vapor deposition [11,12], density gradient ultracentrifugation [13,14], DNA wrapping dispersion [15,16], and gel based chromatography [17,18]) have been proposed to obtain single chirality or pure metallic/semiconducting SWCNTs from as-grown materials, it is still difficult to control the electronic feature separation. In particular, the separation approaches suffer from problems such as structural defects, chemical modification of surfactants onto the sidewalls, and the presence of metallic residues in the resulting SWCNTs. As shown in Fig. 1, the other concepts without surfactants and metallic catalysts can be used to separate and synthesize chirality-controlled SWCNTs directly by using [*n*]cycloparaphenylenes ([*n*]CPPs) [19,20], which are the fundamental unit of armchair type SWCNTs (a-SWCNTs) with a metallic feature. However, there still remains a mismatch between the inner diameters of the SWCNTs and the [*n*]CPPs due to excess pyrolysis of misorientated [*n*]CPPs during the SWCNT growth process. In the current report, we propose a novel route to synthesize SWCNTs with a defined chirality using orientated fullerene guests encapsulated inside the cavity of [*n*]CPP hosts.

Theoretical and experimental studies have revealed that encapsulated fullerenes ex-

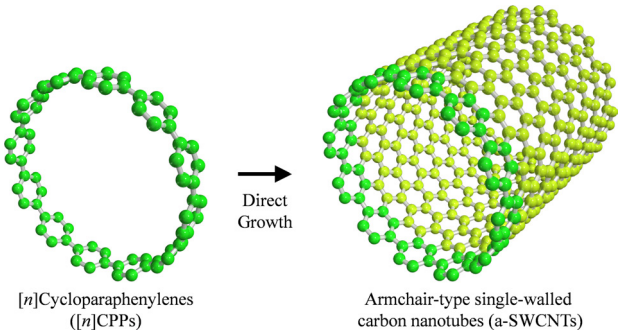

Fig. 1. Chirality-controlled growth concept of a-SWCNTs from [*n*]CPPs.

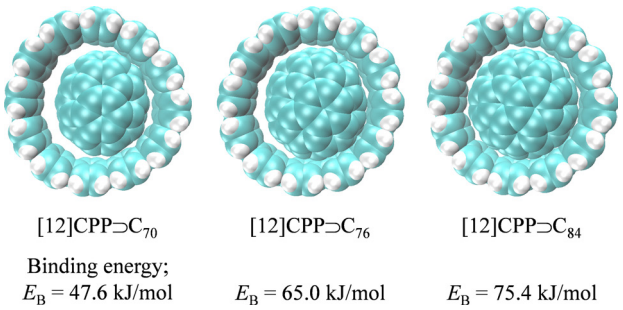

Fig. 2. Optimized structures for the host-guest complexes between [12]CPP and each fullerene (C_{70}, C_{76}, and C_{84}) with each binding energy.

hibit size and shape selectivity due to van der Waals interactions and its electronic states, which provide non-covalent bonds and maintain a structurally stable distance close to that found in graphite interlayers [21-25]. For example, C_{60} with a 0.71 nm diameter was observed to be fully encapsulated into [10]CPPs with a 1.38 nm diameter, although ellipsoidal fullerene of C_{70} with short and long axes (0.71 and 0.80 nm, respectively) could be encapsulated into both [10]CPPs and [11]CPPs due to two different orientations [24,25]. Thus, comfortable distances to coincide with the graphitic interlayer distance (~0.34 nm) [26,27] would be determined by the diameters between CPPs and fullerenes. When [12]CPPs with a diameter of approximately 1.65 nm in [28] were employed as a commercial chemical, C_{84} with a diameter of ~0.84 nm [29] had the possibility of being encapsulated into [12]CPPs because the interlayer distance between the encapsulated C_{84} and [12]CPPs is estimated to be 0.405 nm, which is close to the interlayer distance in graphite, even though we observed a slight mismatch in the interlayer distance of 0.06 nm. In order to estimate the comfortable interlayer distance, calculations were performed utilizing the Troullier-Martins norm-conserving pseudopotentials [30] with the Perdew-Burke-Ernzerhof exchange-coorelation functionals [31] (an energy cutoff of 100 Ry) as implemented in the CPMD code [32]. The results suggested that different from other fullerenes (e.g., C_{70} and C_{76}), C_{84} was likely to be encapsulated into [12]CPPs because C_{84} had the highest binding energy between the host-guest complexes after structural optimization (Fig. 2). In particular, C_{70} and C_{76} were not suitable to be encapsulated into the cavity of [12]CPP because of a large interlayer distance ranging from 0.51 to 0.48 nm, whereas C_{84} was exactly centered on the cavity and had a narrow interlayer distance of approximately 0.43 nm. Therefore, we employed commercial chemicals of [12]CPPs and used C_{84} as the guest rather than C_{70} and C_{76} which had smaller diameters of 0.71–0.8 and about 0.8 nm [24,25,29] (i.e., larger mismatched interlayer distances of >0.425 nm than that of C_{84}).

In this study, [12]CPPs encapsulating fullerenes ([12]CPPs $\supset C_{70}$, $\supset C_{76}$, and $\supset C_{84}$) were pyrolyzed via hot-filament heat treatment in a vacuum with focused ultraviolet (UV) laser irradiation, and we resolved the growth problems of SWCNTs and achieved a narrow diameter distribution. In order to promote rapid growth of SWCNTs with a narrow diameter distribution, anhydrous ethanol vapor as a carbon source was flowed along with Ar carrier gas into the furnace during the heat treatment. The obtained samples were characterized by scanning electron microcopy (SEM)/transmission electron microscopy (TEM), Raman spectroscopy, and molecular dynamics (MD) simulations.

2. Experimental

2.1. Synthesis of SWCNTs from [12]cycloparaphenylenes (CPPs)

Silicon substrates (1 cm × 1 cm) with a (100) plane on the surface were cleaned by dipping them in a hydrofluoric acid solution (concentration of 46.0–48.0%; Kanto Chemical Co., Inc., Japan) at room temperature to remove surface oxides and washing them repeatedly with distilled water until the pH became neutral. To prepare atomically flat surfaces on silicon substrates, the treated substrates were dipped into a 50 mmol L^{-1} ammonium sulfite solution and washed five times with distilled water, followed by drying at 100°C under an Ar gas flow. [12]CPP solutions were prepared by dissolving [12]CPPs (purity of >90.0%, Tokyo Chemical Industry Co., Ltd.) without and with fullerenes (1:1 by a mole ratio) in anhydrous toluene (purity of 99.8%, Sigma-Aldrich Co., Ltd.) so as to correspond to 0.5 mmol L^{-1}; 5 μL of the solution was dropped onto an Si substrate and spin-coated at 1500 rpm for 1 min, followed by drying under an Ar gas flow. An additional drop of 5 μL of [12]CPP solution without fullerenes was put onto the substrate by the above-mentioned procedures. The prepared substrate was placed into a

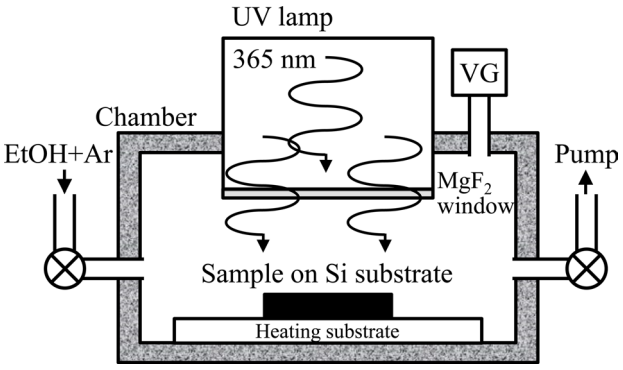

Fig. 3. Schematic illustration of a vacuum chamber with an UV irradiation system through a transparent MgF_2 window. VG, vacuum gauge.

furnace and heat-treated at 500°C for 15 min in a vacuum with focused UV laser irradiation (Fig. 3). During the heat treatment, anhydrous ethanol (water content of <50 ppm, Kanto Chemical Co., Inc.) vapor as a carbon source was flowed along with Ar carrier gas into the furnace by vacuum pressure to facilitate the growth of SWCNTs.

2.2. Structural analysis

The macro-morphology of the resulting samples on an Si substrate was observed by an SEM (VE-8800, Keyence Co., Japan) with an accelerating voltage of 10 kV. After SEM observations, the samples on the substrate were ultrasonicated for 5 min in an ethanol solution to free the nanotubes into the suspension. The supernatant was dropped onto a carbon-coated TEM grid and dried at about 80°C under an Ar gas flow. The structures were observed by TEM (JEM-2100F, JEOL Ltd., Japan) at an accelerating voltage of 200 kV in a high vacuum. Raman spectra of the resulting samples on an Si substrate were collected using a Raman measurement system (NRS-7100, JASCO Co., Ltd.) with a 532 nm green laser line and ×100 objective lenses. All spectra were calibrated with Si-Si vibrations at 520 cm^{-1} as an internal standard.

2.3. Computational analysis during the SWCNT growth process

To theoretically investigate the SWCNT growth process from [12]CPPs on an Si substrate with a (100) plane, we built three [12]CPP models in which a series of fullerenes was encapsulated inside the cavity of [12]CPPs, in addition to a [12]CPP model without fullerenes. These models were built using a software package for computational chemistry and molecular modelling tools: Hyperchem ver. 7.0 (Hypercube Inc., USA) [33]. These models were initial structures for MD simulations which were run in an MD simulator: LAMMPS for 30 ps with 0.1 fs time steps and 500°C under periodic boundary conditions in all directions. The potentials for MD simulations employed were ReaxFF sets, which have been successfully used to determine the structures of various organic/inorganic materials including hydrocarbons [34], graphenes [35], amines [36], and silicon/silicon oxides [37,38].

3. Results and Discussion

Structural morphologies of all the samples were characterized by SEM and TEM. Low-magnification SEM images (Fig. 4a, c, e) revealed fiber morphologies in all samples even though there was a large number of rod-like structures with wide diameters only in the pyrolyzed sample from [12]CPPs⊃C_{70} (SW70). The rod-like crystals of C_{70} can be produced from toluene-alcohol solution containing fullerene via liquid-liquid interfacial precipitation [39,40]. Thus, the rod-like structures in the SEM image (Fig. 4a) are thought to be C_{70} crystals because we employed toluene containing C_{70} as well as ethanol vapor to produce SWCNTs. On the other hand, as shown in the high-magnification SEM images (Fig. 4b, d, f), the number of aggregated particles decreased and the amount of fiber morphology increased with

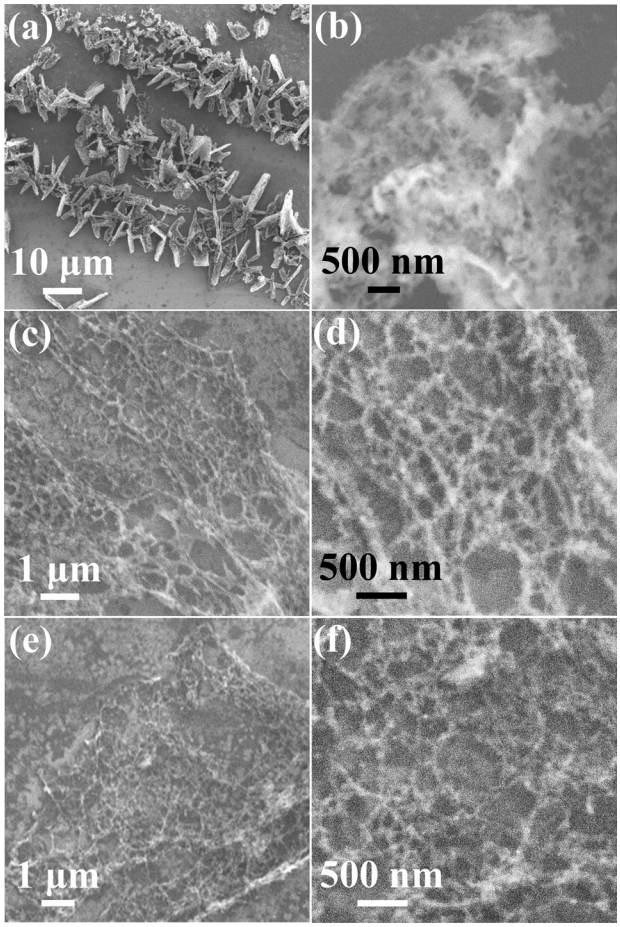

Fig. 4. SEM images of (a, b) SW70, (c, d) SW76, and (e, f) SW84.

an increasing diameter of the fullerenes. This indicated that the morphology of the SWCNTs was dependent on the diameter of fullerene guests as templates to transform [12]CPP hosts to SWCNTs. Unfortunately, the TEM images of SW70 (Fig. 5a-c) revealed that amorphous fibers were formed with diameters ranging from 5 to 30 nm and no tubular structures were derived from SWCNTs. However, the pyrolyzed [12]CPPs⊃C_{76} (SW76) and [12]CPPs⊃C_{84} (SW84) were observed in TEM images (Fig. 5d-i) to have both amorphous and tubular structures without any obvious difference between their samples even though the fullerenes and/or the decomposed carbon molecules remained in the inner and outer tubes. The diameter distribution of a pyrolyzed [12]CPP⊃C_{84} (SW84) is shown in Fig. 6, which was derived by counting the number of tubular structures (100 tubes), except for the amorphous structures. The measured diameters of the tubular structures ranged from 1.5 to 1.7 nm (Fig. 6) corresponding to the diameter range of [12]CPPs. In addition, the diameter range had a narrower distribution compared with the range of [19] without any fullerene templates, which suggests that a comfortable fullerene encapsulated inside the cavity of [12]CPP can determine the pyrolyzed positions between [12]CPPs because of π-π interactions between [12]CPPs and the fullerenes. On the other hand, the yield of tubular structures could not be determined because of the small amount of the obtained CNTs. The

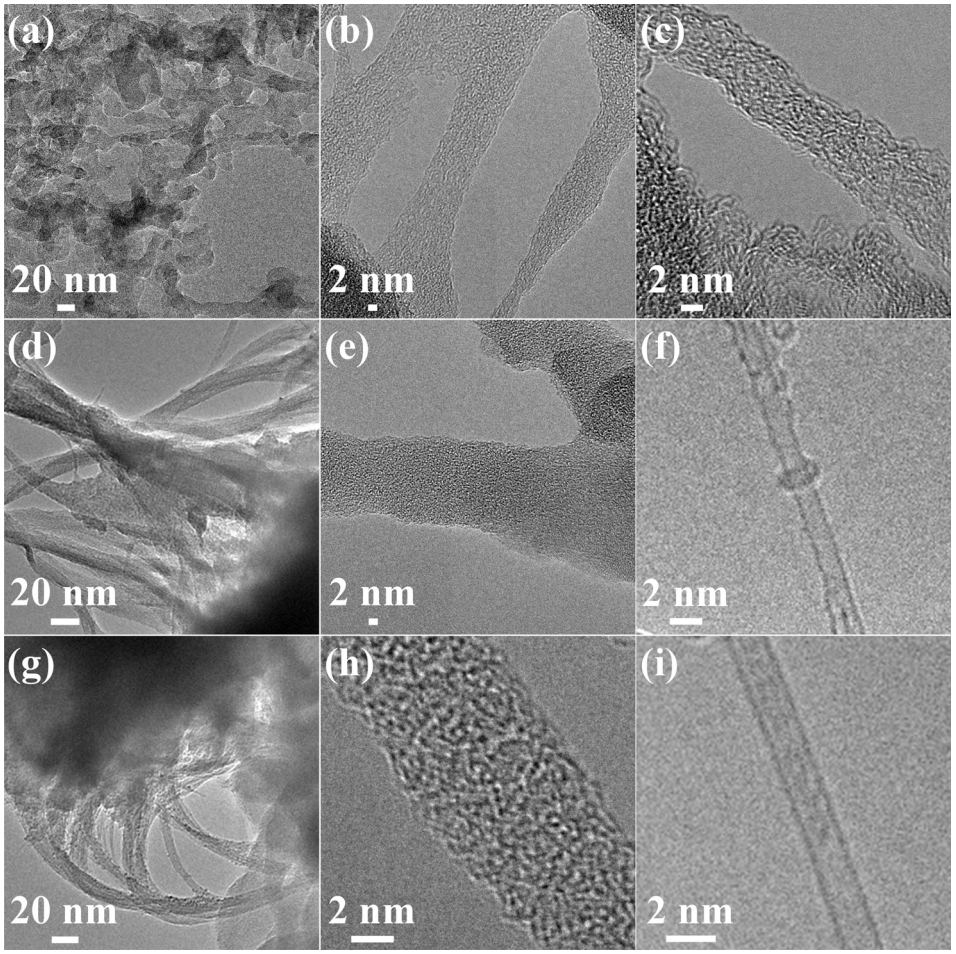

Fig. 5. TEM images of (a-c) SW70, (d-f) SW76, and (g-i) SW84.

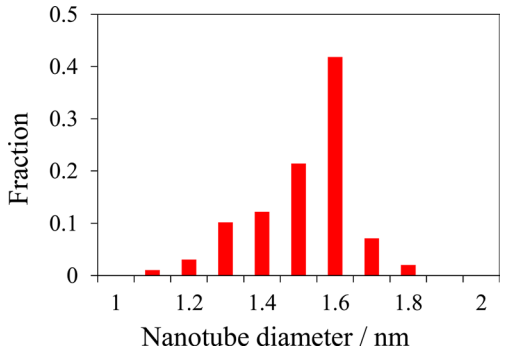

Fig. 6. Diameter distribution histogram for SW86. It is difficult to count the number of SWCNTs within our samples because the amount of tubular structures is really small and the nanotubes were covered by a large amount of amorphous carbon.

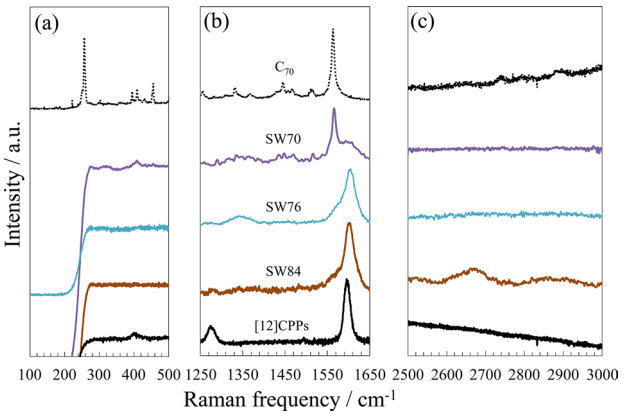

Fig. 7. (a) Raman spectra of SW70, SW76, and SW84 compared with C_{70} and [12]CPPs. Note that the radial breathing mode of the SWCNTs is generally observed in the range from 100 to 400 cm^{-1}. (b) D- and G-bands are observed at approximately 1350 and 1600 cm^{-1}, respectively. (c) The G′-band is identified in the range of 2500 to 2800 cm^{-1}.

above-mentioned results indicated that size-selective encapsulation of fullerenes by [12]CPPs influenced the growing structures and the tubular diameters.

Interestingly, Raman spectra (Fig. 7a) of resulting samples with tubular structures did not clearly display the radial breathing mode [41] in which SWCNTs symmetrically undergo a radial displacement because of a small amount of SWCNTs on a silicon substrate. SW76 and SW84 in Fig. 7a show the same spectra, which are clearly different from those of C_{70} and [12]CPPs. In addition, their Raman spectra in Fig. 7b showed two main peaks

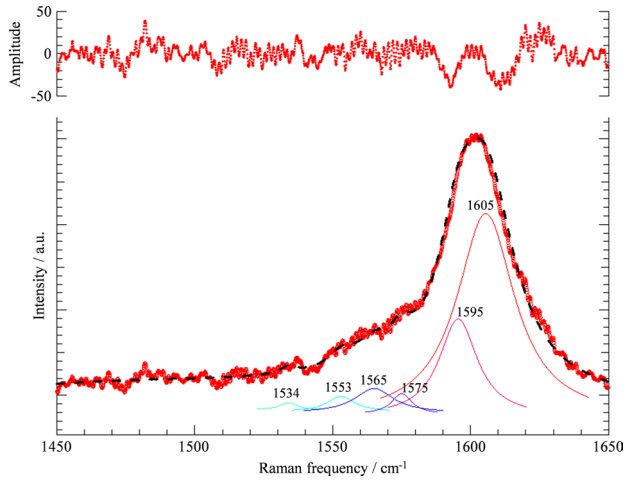

Fig. 8. Raman spectrum for SW84 associated with the C-C stretching modes of SWCNTs obtained using the 532 nm laser line. The colour curves represent the individual Lorentzian functions and the dotted curve represents the fit to the experimental data of red circles. The difference patterns between the fitting curves and the experimental data is given on top of the Raman spectrum.

[41], namely, a low intensity D-band (defect-induced mode) at 1350 cm^{-1} and a high intensity G-band (graphite mode) at 1601 cm^{-1}. The spectra of the G mode for SW76 and SW84 shifted slightly toward values higher than that of [12]CPPs. This upward shift indicated formation of decomposed molecules from fullerene and/or [12]CPPs because SW70 with an amorphous structure displayed a peak at 1601 cm^{-1}. The Raman spectra of SW70 showed a peak at approximately 1560 cm^{-1}, which corresponds to the rod-like crystals of C_{70} in the SEM and TEM images (Figs. 4a,b and 5a-c). On the other hand, the Raman spectra of SW76 and SW84 displayed a broadened shoulder peak at 1574 cm^{-1} along with other peaks. As shown in Fig. 8, the Raman peaks of SW84 in the range between 1540 and 1600 cm^{-1} could be deconvoluted into six different peaks at 1534, 1553, 1565, 1575, 1595, and 1605 cm^{-1} using a Lorentzian distribution function. Their Raman features are very similar to those of semiconducting SWCNTs (s-SWCNTs) [42], even though they are upshifted about 5 cm^{-1}. Such a change can be explained by the difference in the electronic density of states (DOS) for the s-SWCNTs coming from their diameter range of 1.0 to 1.6 nm. In addition, the broad G'-band in the range between 2600 and 2700 cm^{-1} is clearly observed only for SW84 (Fig. 7c). The G'-band could be deconvoluted into two peaks, suggesting the presence of two different van Hove singularities from s-SWCNTs [43].

The SWCNTs obtained were thought to be semiconductors due to the presence of decomposed paraphenylenes. In reactive MD simulations, [12]CPPs without fullerenes on an Si substrate were decomposed into oligoparaphenylenes (OPPs) through

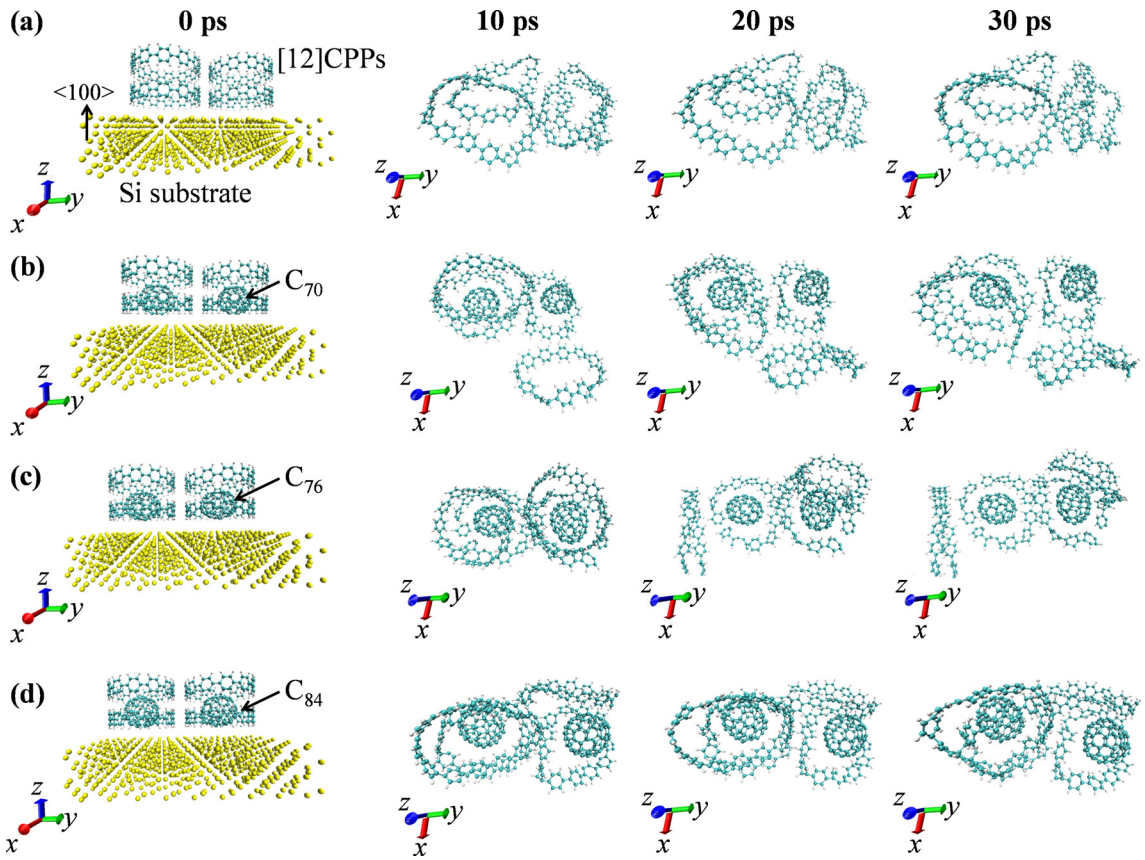

Fig. 9. Snapshots of the SWCNT growth process from [12]CPPs (a) without and with fullerenes: (b) C_{70}, (c) C_{76}, and (d) C_{84} on an Si substrate with the (100) plane in the *z* axis. To clearly display structural changes in [12]CPPs, the Si substrate was not shown after 10 ps.

vacuum heat treatment (Fig. 9a), thus facilitating the misorientated growth of SWCNTs. Conversely, [12]CPPs⊃C_{84} were decomposed into a few OPPs by partially maintaining orientated ring structures due to π-π interactions between [12]CPPs and fullerenes (Fig. 9b-d). This indicates that the encapsulated fullerenes within [12]CPPs possess higher thermal stability than [12]CPPs without any fullerene because of the strong π-π interaction between [12]CPPs and fullerenes, even though there was a slight decomposition of [12]CPPs in their models after 20 ps. According to the proposed growth models [19,20], OPPs obtained from the ring-cleavage reactions of CPP radicals could generate a template for non a-SWCNTs because they induced dimerization or oligomerization during heat treatment. Therefore, the obtained sample was thought to be predominantly s-SWCNTs, even though perfect control of diameter/chirality was limited by the formation of OPPs.

4. Conclusions

We proposed an efficient synthetic method for producing SWCNTs with a narrow diameter distribution by selecting the diameter of fullerene guests encapsulated inside the cavity of CPP hosts. The obtained SWCNTs were thought to have predominantly semiconducting features by Raman spectroscopic analysis and MD simulations because of the formation of OPPs under vacuum heat treatment and promotion of thermal fusion between the misorientated CPPs. If ring structures of CPPs are completely maintained during the heat treatment, we might be able to obtain SWCNTs with conductive features bacause CPPs are the fundamental unit of armchair type nanotubes with a metallic feature. Therefore, with this new approach it might be possible to design their electronic features, thereby opening up new potential applications. However, for future study, it will be necessary to develop a method to increase the amount of SWCNTs.

Conflict of Interest

No potential conflict of interest relevant to this article was reported.

Acknowledgements

T.T. acknowledges support through a Grant-in-Aid for challenging Exploratory Research (No. 15K13947) and Toyota Physical and Chemical Research Institute Scholar Project. T.T. would like to thank the Naito Science & Engineering Foundation for their partial support. Y.A.K. acknowledges the financial support from a grant from the National Research Foundation of Korea (NRF) funded by the Korean government (MSIP) (No. NRF-2017R1A2A1A17069771) and from the Nano · MaterialTechnology Development Program through the NRF funded by the Ministry of Science, ICT and Future Planning of Korea (2016M3A7B4021149).

References

[1] Hwang I, Jung HJ, Cho SH, Jo SS, Choi YS, Sung JH, Choi JH, Jo MH, Park C. Efficient room-temperature near-infrared detection with solution-processed networked single wall carbon nanotube field effect transistors. Small, **10**, 653 (2014). https://doi.org/10.1002/smll.201301582.

[2] Yoon J, Shin G, Kim J, Moon YS, Lee SJ, Zi G, Ha JS. Fabrication of stretchable single-walled carbon nanotube logic devices. Small, **10**, 2910 (2014). https://doi.org/10.1002/smll.201303779.

[3] Meyyappan M. Carbon nanotube-based chemical sensors. Small, **12**, 2118 (2016). https://doi.org/10.1002/smll.201502555.

[4] Zhu Z. An overview of carbon nanotubes and graphene for biosensing applications. Nano-Micro Lett, **9**, 25 (2017). https://doi.org/10.1007/s40820-017-0128-6.

[5] Martínez-Sarti L, Pertegás A, Monrabal-Capilla M, Gilshteyn E, Varjos I, Kauppinen EI, Nasibulin AG, Sessolo M, Bolink HJ. Flexible light-emitting electrochemical cells with single-walled carbon nanotube anodes. Org Electron, **30**, 36 (2016). https://doi.org/10.1016/j.orgel.2015.12.011.

[6] Kanninen P, Luong ND, Sinh LH, Anoshkin IV, Tsapenko A, Seppälä J, Nasibulin AG, Kallio T. Transparent and flexible high-performance supercapacitors based on single-walled carbon nanotube films. Nanotechnology, **27**, 235403 (2016). https://doi.org/10.1088/0957-4484/27/23/235403.

[7] Yang MH, Choi BG. Preparation of gold nanoparticle/single-walled carbon nanotube nanohybrids using biologically programmed peptide for application of flexible transparent conducting films. Carbon Lett, **20**, 26 (2016). https://doi.org/10.5714/cl.2016.20.026.

[8] Nicola FD, Salvato M, Cirillo C, Crivellari M, Boscardin M, Passacantando M, Nardone M, Matteis FD, Motta N, Crescenzi MD, Castrucci P. 100% internal quantum efficiency in polychiral single-walled carbon nanotube bulk heterojunction/silicon solar cells. Carbon, **114**, 402 (2017). https://doi.org/10.1016/j.carbon.2016.12.050.

[9] Bhatia R, Ujjain SK. Soluble single-walled carbon nanotubes for photovoltaics. Mater Lett, **190**, 165 (2017). https://doi.org/10.1016/j.matlet.2017.01.008.

[10] Zhang G, Qi P, Wang X, Lu Y, Li X, Tu R, Bangsaruntip S, Mann D, Zhang L, Dai H. Selective etching of metallic carbon nanotubes by gas-phase reaction. Science, **314**, 974 (2006). https://doi.org/10.1126/science.1133781.

[11] Sanchez-Valencia JR, Dienel T, Gröning O, Shorubalko I, Mueller A, Jansen M, Amsharov K, Ruffieux P, Fasel R. Controlled synthesis of single-chirality carbon nanotubes. Nature, **512**, 61 (2014). https://doi.org/10.1038/nature13607.

[12] Yang F, Wang X, Zhang D, Yang J, Luo D, Xu Z, Wei J, Wang JQ, Xu Z, Peng F, Li X, Li R, Li Y, Li M, Bai X, Ding F, Li Y. Chirality-specific growth of single-walled carbon nanotubes on solid alloy catalysts. Nature, **510**, 522 (2014). https://doi.org/10.1038/nature13434.

[13] Arnold MS, Green AA, Hulvat JF, Stupp SI, Hersam MC. Sorting carbon nanotubes by electronic structure using density differentiation. Nat Nanotechnol, **1**, 60 (2006). https://doi.org/10.1038/nnano.2006.52.

[14] Green AA, Hersam MC. Nearly single-chirality single-walled carbon nanotubes produced via orthogonal iterative density gradient ultracentrifugation. Adv Mater, **23**, 2185 (2011). https://doi.

org/10.1002/adma.201100034.

[15] Tu X, Manohar S, Jagota A, Zheng M. DNA sequence motifs for structure-specific recognition and separation of carbon nanotubes. Nature, **460**, 250 (2009). https://doi.org/10.1038/nature08116.

[16] Tu X, Walker ARH, Khripin CY, Zheng M. Evolution of DNA sequences toward recognition of metallic armchair carbon nanotubes. J Am Chem Soc, **133**, 12998 (2011). https://doi.org/10.1021/ja205407q.

[17] Liu H, Nishide D, Tanaka T, Kataura H. Large-scale single-chirality separation of single-wall carbon nanotubes by simple gel chromatography. Nat Commun, **2**, 309 (2011). https://doi.org/10.1038/ncomms1313.

[18] Yomogida Y, Tanaka T, Zhang M, Yudasaka M, Wei X, Kataura H. Industrial-scale separation of high-purity single-chirality single-wall carbon nanotubes for biological imaging. Nat Commun, **7**, 12056 (2016). https://doi.org/10.1038/ncomms12056.

[19] Omachi H, Nakayama T, Takahashi E, Segawa Y, Itami K. Initiation of carbon nanotube growth by well-defined carbon nanorings. Nat Chem, **5**, 572 (2013). https://doi.org/10.1038/nchem.1655.

[20] Okada K, Yagi A, Segawa Y, Itami K. Synthesis and properties of [8]-, [10]-, [12]-, and [16]cyclo-1,4-naphthylenes. Chem Sci, **8**, 661 (2017). https://doi.org/10.1039/C6SC04048A.

[21] Hermann J, Alfè D, Tkatchenko A. Nanoscale π–π stacked molecules are bound by collective charge fluctuations. Nat Commun, **8**, 14052 (2017). https://doi.org/10.1038/ncomms14052.

[22] Yuan K, Dang JS, Guo YJ, Zhao X. Theoretical prediction of the host–guest interactions between novel photoresponsive nanorings and C_{60}: a strategy for facile encapsulation and release of fullerene. J Comput Chem, **36**, 518 (2015). https://doi.org/10.1002/jcc.23824.

[23] Rio J, Erbahar D, Rayson M, Briddon P, Ewels CP. Cyclotetrahalo-p-phenylenes: simulations of halogen substituted cycloparaphenylenes and their interaction with C_{60}. Phys Chem Chem Phys, **18**, 23257 (2016). https://doi.org/10.1039/C6CP03376H.

[24] Iwamoto T, Watanabe Y, Sadahiro T, Haino T, Yamago S. Size-selective encapsulation of C_{60} by [10]cycloparaphenylene: formation of the shortest fullerene-peapod. Angew Chem Int Ed, **50**, 8342 (2011). https://doi.org/10.1002/anie.201102302.

[25] Iwamoto T, Watanabe Y, Takaya H, Haino T, Yasuda N, Yamago S. Size- and orientation-selective encapsulation of C_{70} by cycloparaphenylenes. Chem Eur J, **19**, 14061 (2013). https://doi.org/10.1002/chem.201302694.

[26] Rao CNR, Satishkumar BC, Govindaraj A, Nath M. Nanotubes. ChemPhysChem, **2**, 78 (2001). https://doi.org/10.1002/1439-7641(20010216)2:2<78::AID-CPHC78>3.0.CO;2-7.

[27] Kim YA, Yang KS, Muramatsu H, Hayashi T, Endo M, Terrones M, Dresselhaus MS. Double-walled carbon nanotubes: synthesis, structural characterization, and application. Carbon Lett, **15**, 77 (2014). https://doi.org/10.5714/CL.2014.15.2.077.

[28] Segawa Y, Miyamoto S, Omachi H, Matsuura S, Šenel P, Sasamori T, Tokitoh N, Itami K. Concise synthesis and crystal structure of [12]cycloparaphenylene. Angew Chem Int Ed, **50**, 3244 (2011). https://doi.org/10.1002/anie.201007232.

[29] Bandow S, Takizawa M, Kato H, Okazaki T, Shinohara H, Iijima S. Smallest limit of tube diameters for encasing of particular fullerenes determined by radial breathing mode Raman scattering. Chem Phys Lett, **347**, 23 (2001). https://doi.org/10.1016/S0009-2614(01)01020-X.

[30] Troullier N, Martins JL. Efficient pseudopotentials for plane-wave calculations. Phys Rev B, **43**, 1993 (1991). https://doi.org/10.1103/PhysRevB.43.1993.

[31] Perdew JP, Burke K, Ernzerhof M. Generalized gradient approximation made simple. Phys Rev Lett, **77**, 3865 (1996). https://doi.org/10.1103/PhysRevLett.77.3865.

[32] CPMD ver 3.11.1, IBM Co., 2000-2017. Available from: http://www.cpmd.org.

[33] Hyerchem Release ver. 7.03 for Windows, Hypercube Inc., 2002. Available from: http://www.hyper.com.

[34] van Duin ACT, Dasgupta S, Lorant F, Goddard III WA. ReaxFF: a reactive force field for hydrocarbons. J Phys Chem A, **105**, 9396 (2001). https://doi.org/10.1021/jp004368u.

[35] Yoon K, Rahnamoun A, Swett JL, Iberi V, Cullen DA, Vlassiouk IV, Belianinov A, Jesse S, Sang X, Ovchinnikova OS, Rondinone AJ, Unocic RR, van Duin ACT. Atomistic-scale simulations of defect formation in graphene under noble gas ion irradiation. ACS Nano, **10**, 8376 (2016). https://doi.org/10.1021/acsnano.6b03036.

[36] Furman D, Dubnikova F, van Duin ACT, Zeiri Y, Kosloff R. Reactive force field for liquid hydrazoic acid with applications to detonation chemistry. J Phys Chem C, **120**, 4744 (2016). https://doi.org/10.1021/acs.jpcc.5b10812.

[37] Wen J, Ma T, Zhang W, Psofogiannakis G, van Duin ACT, Chen L, Qian L, Hu Y, Lu X. Atomic insight into tribochemical wear mechanism of silicon at the Si/SiO_2 interface in aqueous environment: molecular dynamics simulations using ReaxFF reactive force field. Appl Surf Sci, **390**, 216 (2016). https://doi.org/10.1016/j.apsusc.2016.08.082.

[38] Yeon J, van Duin ACT, Kim SH. Effects of water on tribochemical wear of silicon oxide interface: molecular dynamics (MD) study with reactive force field (ReaxFF). Langmuir, **32**, 1018 (2016). https://doi.org/10.1021/acs.langmuir.5b04062.

[39] Miyazawa K, Hamamoto K, Nagata S, Suga T. Structural investigation of the C_{60}/C_{70} whiskers fabricated by forming liquid–liquid interfaces of toluene with dissolved C_{60}/C_{70} and isopropyl alcohol. J Mater Res, **18**, 1096 (2003). https://doi.org/10.1557/JMR.2003.0151.

[40] Minato J, Miyazawa K. Solvated structure of C_{60} nanowhiskers. Carbon, **43**, 2837 (2005). https://doi.org/10.1016/j.carbon.2005.06.013.

[41] Rao AM, Richter E, Bandow S, Chase B, Eklund PC, Williams KA, Fang S, Subbaswamy KR, Menon M, Thess A, Smalley RE, Dresselhaus G, Dresselhaus MS. Diameter-selective raman scattering from vibrational modes in carbon nanotubes. Science, **275**, 187 (1997). https://doi.org/10.1126/science.275.5297.187.

[42] Pimenta MA, Marucci A, Brown SDM, Matthews MJ, Rao AM, Eklund PC, Smalley RE, Dresselhaus G, Dresselhaus MS. Resonant Raman effect in single-wall carbon nanotubes. J Mater Res, **13**, 2396 (1998).

[43] Dresselhaus MS, Dresselhaus G, Saito R, Jorio A. Raman spectroscopy of carbon nanotubes. Phys Rep, **409**, 47 (2005). https://doi.org/10.1016/j.physrep.2004.10.006.